

Embryonic origin and Hox status determine progenitor cell fate during adult bone regeneration

Philipp Leucht, Jae-Beom Kim, Raimy Amasha, Aaron W. James, Sabine Girod and Jill A. Helms*

The fetal skeleton arises from neural crest and from mesoderm. Here, we provide evidence that each lineage contributes a unique stem cell population to the regeneration of injured adult bones. Using *Wnt1Cre::Z/EG* mice we found that the neural crest-derived mandible heals with neural crest-derived skeletal stem cells, whereas the mesoderm-derived tibia heals with mesoderm-derived stem cells. We tested whether skeletal stem cells from each lineage were functionally interchangeable by grafting mesoderm-derived cells into mandibular defects, and vice versa. All of the grafting scenarios, except one, healed through the direct differentiation of skeletal stem cells into osteoblasts; when mesoderm-derived cells were transplanted into tibial defects they differentiated into osteoblasts but when transplanted into mandibular defects they differentiated into chondrocytes. A mismatch between the Hox gene expression status of the host and donor cells might be responsible for this aberration in bone repair. We found that initially, mandibular skeletal progenitor cells are Hox-negative but that they adopt a *Hoxa11*-positive profile when transplanted into a tibial defect. Conversely, tibial skeletal progenitor cells are Hox-positive and maintain this Hox status even when transplanted into a Hox-negative mandibular defect. Skeletal progenitor cells from the two lineages also show differences in osteogenic potential and proliferation, which translate into more robust in vivo bone regeneration by neural crest-derived cells. Thus, embryonic origin and Hox gene expression status distinguish neural crest-derived from mesoderm-derived skeletal progenitor cells, and both characteristics influence the process of adult bone regeneration.

KEY WORDS: Neural crest, Mesoderm, Periosteum, Osteoblast, Chondrocyte, Graft, Mouse

INTRODUCTION

Bone is a self-renewing tissue (Seeman and Delmas, 2006). Mammalian bone has such a high turnover rate that the bulk of skeletal tissues are completely replaced each decade. This inherent regenerative capacity suggests that the skeleton must harbor a reservoir of undifferentiated progenitor cells that give rise to new bone. One source of these skeletal progenitor cells is the periosteum, which harbors proliferating cells that can differentiate into either chondrocytes or osteoblasts, which deposit new mineralized matrix. This matrix is continuously resorbed by osteoclasts, which in turn stimulates new osteoblastogenesis. Through this mechanism, the skeleton is continually reconstituted throughout the life of an organism.

Bone formation and resorption occur in all bones, and at a macroscopic level the skeletal tissues in the body and those in the head are indistinguishable. There is, however, one unique characteristic: the facial skeleton is derived exclusively from cranial neural crest, whereas the rest of the skeleton is derived from mesoderm (Noden, 1982; Couly et al., 1993). This raises a fundamental question: are there two sub-populations of skeletal stem cells or is there a single population that is responsible for the continual regeneration of bone?

One way to address this question is to evaluate how mesoderm-derived and neural crest-derived bones undergo repair because, unlike the life-long process of remodeling, injury-induced bone regeneration occurs within a compressed time frame and in a precise location. The cellular and molecular machinery responsible for adult bone formation in these conditions is, however, identical (Ferguson et al., 1998; Colnot et al., 2003; Gerstenfeld et al., 2003).

We used a cell-labeling strategy to indelibly mark neural crest-derived cells and mesoderm-derived cells, and then produced skeletal injuries in a neural crest-derived bone, the mandible, and in a mesoderm-derived bone, the tibia. In evaluating the healing phase we uncovered a neural crest stem cell reservoir that contributes cells exclusively to the regeneration of neural crest-derived skeletal elements. We also found that neural crest-derived and mesoderm-derived bones heal through the selective recruitment of cells from their own embryonic origins. We directly tested the extent to which these populations are interchangeable in a clinically relevant model of bone grafting. Our results indicate that skeletal stem cells have ‘positional memory’, which influences how the cells behave when grafted into ectopic locations.

MATERIALS AND METHODS

Animals

All experiments were performed in accordance with Stanford University Animal Care and Use Committee guidelines. Transgenic mice, expressing *Cre* recombinase under the control of the *Wnt1* promoter (Danielian et al., 1998), were mated to *Z/EG* mice (Novak et al., 2000). Prior to expression of *Cre* recombinase, cells from all stages of *Z/EG* mice exhibit constitutive expression of β -galactosidase, but in the presence of *Cre* recombinase the expression of β -galactosidase is replaced by expression of GFP.

Periosteal harvest and surgical implantation

Periosteum was harvested from the mandible and tibia by careful dissection from the bones followed by rapid washing in cold PBS and transplantation into drill-hole defects in skeletally mature, male FVB mice. To conduct the tibial transplantation, an incision was made over the right anterior-proximal tibia and the tibial surface was exposed while preserving the periosteal surface. A drill hole was created through a single cortex in the midline of the tibia distal to the tibial tuberosity with a dental drill (15,000 rpm) using a 1.0 mm drill bit (Drill Bit City, Chicago, IL). The far cortex was neither penetrated nor touched by the drill. The donor GFP periosteum was then placed into the host defect. After irrigation, the previously mobilized muscle flap was placed over the defect and sutured to the skeletal wound using 7-0 Vicryl (Ethicon, Somerville, NJ). Skin was closed using 7-0 Prolene

Department of Surgery, Division of Plastic and Reconstructive Surgery, Stanford University School of Medicine, Stanford, CA 94305, USA.

*Author for correspondence (e-mail: jhelms@stanford.edu)

(Ethicon). In the mandible, an incision was made horizontally across the right buccinator muscle and kept open with a retractor. A 1.0 mm drill hole was made into the exposed ramus of the right mandible without creating root damage to the underlying teeth. GFP-labeled periosteum was then placed into the defect, the buccinator muscle approximated and the incision sutured with 7-0 Prolene.

The experimental design allowed for four distinct combinations of transplantation experiments: (1) mandibular GFP-positive periosteum into mandible FVB defect; (2) mandibular GFP-positive periosteum into tibial FVB defect; (3) tibial GFP-positive periosteum into tibial FVB defect; and (4) tibial GFP-positive periosteum into mandible FVB defect.

Following surgery, mice received adequate analgesia and were allowed to ambulate freely (Clifford, 1984). Five mice of each of the four transplant combinations were sacrificed at 7, 10, 15 and 21 days post-surgery. Additionally, five mice with mandibular and tibial defects were sacrificed at each time point. Representative samples were selected for analysis.

Tissue processing, histology and immunohistochemistry

Limbs and mandibles were dissected and processed for paraffin embedding. Sections (8 μ m) were collected on Superfrost-plus slides (Fisher Scientific, Pittsburgh, PA) for histology using a modification of Movat's Pentachrome staining (blue to black, nuclei; red, cytoplasm; red, elastic fibers; yellow, collagen and mineralized bone matrix; blue-green, osteoid or mineralized cartilage; light-blue, cartilage) (Sheehan and Hrapchak, 1980). Immunostaining was performed as described (Colnot et al., 2003; Leucht et al., 2007). Antibodies included green fluorescent protein (GFP; Abcam, Cambridge, MA), platelet endothelial cell adhesion molecule (PECAM; Pharmingen, San Jose, CA), proliferating cell nuclear antigen (PCNA; Zymed, San Francisco, CA) and *Hoxa11* (Abcam). TRAP staining of osteoclasts was performed as described (Colnot et al., 2005). For X-Gal staining, tissues were embedded in OCT, cryosectioned and then stained with X-Gal overnight at 37°C (Kim et al., 2007b).

Histomorphometric measurements

The 1.0 mm circular mono-cortical defect was represented across ~100 tissue sections, each of which was 10 μ m thick. Out of those 100 sections, we used a minimum of 20 sections to quantify the amount of new bone. Sections were stained with Aniline Blue to label osteoid matrix. Digital images were analyzed with Adobe Photoshop CS2 software. In a fixed region of interest (ROI), Aniline Blue-positive pixels were selected using the Magic Wand tool set to a color tolerance of 60 that highlighted pixels with a range of blue that corresponded precisely with the histological appearance of osseous tissue. Cortical surfaces or bone fragments were manually deselected. The total number of Aniline Blue-positive pixels was recorded, then pixel counts from individual sections were averaged for each sample and differences within and among treatment groups were calculated based on these averages.

In situ hybridization

Hybridization was performed using digoxigenin-labeled probes complementary to mouse cDNAs for *Wnt1*, *Hoxa11* and *Hoxa13* (Open Biosystems, Huntsville, AL) as described (Albrecht et al., 1997).

In vivo image analyses

Bioluminescence imaging was performed using an IVIS 200 (Caliper Life Sciences, Alameda, CA). Light outputs were quantified using LivingImage software version 2.5 (Xenogen, Alameda, CA) as an overlay on Igor Pro imaging analysis software (WaveMetrics, Portland, OR). The final light output, in photons/second/cm²/steradian, was normalized to the integration time, the distance from the camera to the animal, the instrument gain, and the solid angle of measurement to provide for cross-platform comparison. Bioluminescence imaging was quantified by creation of circular ROIs over the right proximal tibia.

Periosteum harvest for in vitro experiments

For the in vivo experiments, periosteal cells were harvested from the mandible and tibia of skeletally mature wild-type or β -actin GFP mice. Mice were euthanized, then soft tissues surrounding the bones were removed. Bones were washed in PBS twice, followed by five 10-minute digestions in

2 mg/ml collagenase (Roche, Indianapolis, IN) in DMEM (Gibco and Invitrogen, Carlsbad, CA). Cells from the sixth digestion were resuspended in DMEM containing 10% FBS (Omega Scientific, Tarzana, CA), 1% penicillin/streptomycin, 0.1% gentamycin, followed by plating at equal density. Media were replenished every 2 days. Approximately 1 week from tissue harvest, cells were passaged by trypsinization then used for the following assays.

Cellular proliferation assays

Cells were seeded in 96-well plates at a density of 1000 cells per well and on days 3, 5 and 7 BrdU assays were performed according to the manufacturer's instructions (Roche). Means and standard deviations were calculated. Neural crest-derived periosteal cells were also co-cultured with mesoderm-derived periosteal cells from β -actin GFP mice. Cells were seeded at equal density on chamber slides (Nalge Nunc International, Naperville, IL). After 0, 3, 5 and 7 days, slides were imaged under fluorescent light, digital images were imported into Adobe Photoshop CS2 and GFP-positive and GFP-negative cells were counted by two independent researchers in 10 random ROIs for each time point.

Osteogenic differentiation and assessments

Cells were plated in 24-well plates at a density of 5000 cells per well. After overnight attachment, cells were treated with osteogenic differentiation medium (ODM) containing DMEM, 10% FBS, 100 μ g/ml ascorbic acid, 10 mM β -glycerophosphate and 100 IU/ml penicillin/streptomycin. Media were replenished every 3 days. After 10, 12 and 14 days, Alizarin Red staining was performed.

RNA isolation and quantitative real-time PCR

RNA was isolated (RNeasy Kit, Qiagen, MD), genomic DNA removed (DNA-Free Kit, Ambion, Austin, TX) and the RNA reverse-transcribed (TaqMan Reverse Transcription Reagents, Applied Biosystems, Foster City, CA). Quantitative (q) real-time PCR was carried out using the Applied Biosystems Prism 7900HT Sequence Detection System and Power SYBR Green PCR Master Mix (Applied Biosystems). Specific primers were designed based on PrimerBank (<http://pga.mgh.harvard.edu/primerbank/>) sequence. PCR products were run on a 2% agarose gel to confirm the appropriate size and specificity. Levels of gene expression were determined by normalizing to their *Gapdh* values. All reactions were performed in triplicate; means and standard deviations were calculated.

Statistical analysis

ANOVA two-factor test with replication was used when more than two groups were compared. Welch's two-tailed *t*-test was used when standard deviations between groups were unequal. $P \leq 0.01$ was considered to be significant.

RESULTS

Two populations of skeletal progenitor cells give rise to the adult skeleton

The embryonic facial skeleton is distinguished from the appendicular skeleton by the fact that the former is derived from cranial neural crest and the latter is derived from mesoderm. Do both cell populations contribute skeletal progenitor cells in the adult? Because bone is continually replaced, we could address this question by examining the mandible and tibia of *Wnt1**Cre::Z/EG* transgenic mice. In these mice, *Wnt1* drives the expression of *Cre* recombinase predominantly in derivatives of the neural crest (Chai et al., 2000; Jiang et al., 2000). When crossed with *Z/EG* reporter mice (Novak et al., 2000), the result is GFP labeling of *Wnt1*-expressing neural crest derivatives. Other cell types, including mesodermal derivatives, express β -galactosidase. We examined a variety of adult tissues to verify that this labeling strategy worked.

First, mandibles and tibiae from skeletally mature *Wnt1**Cre::Z/EG* mice were examined. Mandibular osteoblasts and osteocytes exhibited robust GFP immunostaining, indicating their derivation from the neural crest (Fig. 1A). β -galactosidase activity

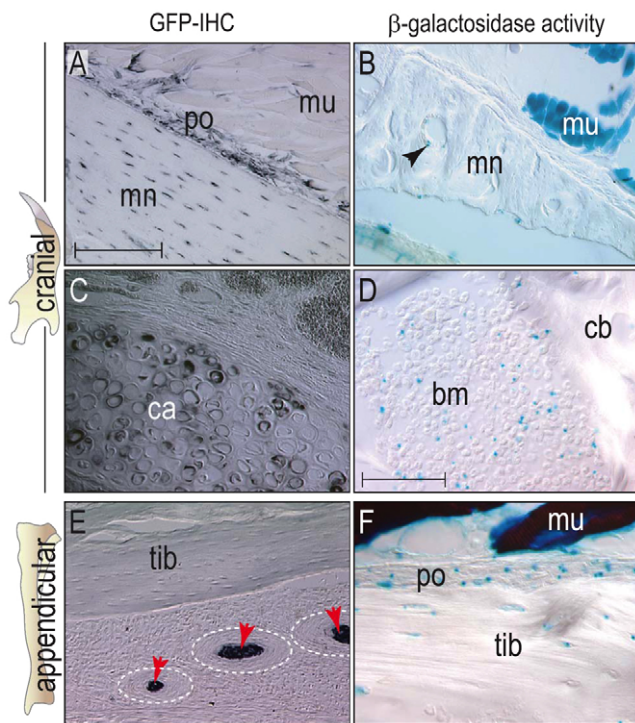


Fig. 1. Cranial and appendicular skeletons are derived from a different embryonic origin. (A,B) In an adult *Wnt1Cre::ZIEG* mouse, mandibular osteocytes and periosteal cells are GFP-positive (neural crest-derived) (A), whereas the adjacent muscle and endothelium (arrowhead) is β -galactosidase-positive (mesoderm-derived) (B). (C,D) Secondary cartilage underlying the skull bone is GFP-positive (C), whereas the hematopoietic system residing in the bone marrow cavity is β -galactosidase-positive (D). (E) The Schwann cells surrounding a peripheral nerve in the hind limb are GFP-positive (arrowheads). (F) Osteocytes and periosteal cells in the tibia stain positive for β -galactosidase. bm, bone marrow; ca, cartilage; cb, cortical bone; mn, mandible; mu, muscle; po, periosteum; tib, tibia. Scale bar: 200 μ m in A-C,E; 100 μ m in D,F.

was absent from mandibular osteoblasts and osteocytes, although the adjacent mesoderm-derived muscle and endothelial cells were positive (Fig. 1B). In secondary cartilages that underlie the skull bones (Le Douarin and Dupin, 1993), neural crest-derived chondrocytes were GFP-positive (Fig. 1C), whereas mesoderm-derived hematopoietic cells (Cumano and Godin, 2007) exhibited β -galactosidase activity (Fig. 1D). In the limbs, neural crest-derived Schwann cells (D'Amico-Martel and Noden, 1983) were GFP-positive, whereas the surrounding mesoderm-derived perineurium (Joseph et al., 2004) was not (Fig. 1E). All tibial osteocytes and periosteum exhibited robust β -galactosidase activity but no GFP immunostaining (Fig. 1E,F). In some tibial sections, we observed β -galactosidase-positive cells adjacent to a morphological structure that ran longitudinally through the bone marrow. Histologically, this structure resembled a nerve with surrounding Schwann cells (data not shown). We only observed 10–20 β -galactosidase-positive cells per longitudinal section of the tibia, however, which was significantly fewer than has been reported elsewhere (Nagoshi et al., 2008).

These data suggest that the skeletal cell lineages established during embryonic development are rigorously maintained throughout the lifetime of an animal. But what if cells become GFP-positive simply because *Wnt1* expression occurs as part of the

normal maturation of an osteoblast? We tested this possibility in two ways: first, we used in situ hybridization for *Wnt1* to see whether the gene was expressed in developing and mature mandibles and tibiae; and second, we performed Cre immunohistochemistry on the same tissues. We detected neither *Wnt1* expression nor Cre immunostaining; consequently, we conclude that Cre-induced recombination occurred during embryonic development and that GFP-positive cells in the facial region were solely the progeny of neural crest cells.

A reservoir of neural crest-derived skeletal progenitor cells exists in adult bones

To ascertain whether neural crest-derived and mesoderm-derived bones use the same skeletal progenitor cell population for their renewal, we generated injuries in the mandible and tibia. These injuries heal through intramembranous ossification and the repair callus has a stereotypical organization (Colnot et al., 2005; Kim et al., 2007a; Kim et al., 2007b; Leucht et al., 2008), which facilitated our subsequent histological, molecular and histomorphometric analyses.

On post-injury day 7, mandibular injuries were filled with new bone (Fig. 2A) and the majority of osteoblasts were immunopositive for GFP ($n=6$; Fig. 2B). β -galactosidase activity was only detectable in adjacent muscle (Fig. 2C). Tibial injuries showed a comparable amount of new bone on day 7 ($n=5$; Fig. 2D), but in contrast to the mandibular defects, this bone was not GFP-positive (Fig. 2E). Instead, tibial osteoblasts exhibited β -galactosidase activity ($n=5$; Fig. 2F). These results indicate that there are two sources of skeletal progenitor cells in an adult animal, and that they can be distinguished from one another based on their embryonic origin. In the tibia, this progenitor pool is derived from β -galactosidase-expressing cells. In the mandible, as well as other neural crest-derived bones of the head, skeletal progenitor cells are derived from GFP-expressing neural crest.

Are neural crest-derived and mesoderm-derived skeletal progenitor cells interchangeable?

The mandible and the tibia form from separate embryonic lineages and our data show that they remodel and heal via these same separate populations. But are these cell populations functionally different? One way to directly test whether they were interchangeable was to perform heterotopic grafts, in which mesoderm-derived skeletal progenitor cells were implanted into a mandibular injury site and neural crest-derived skeletal progenitor cells were implanted into a tibial defect. Before undertaking this experiment, however, we had to ascertain that cells could survive the transplantation procedure and engraft at the injury site. We used bone marrow stromal cells because of their abundance and relative ease of harvesting, and isolated them from *L2G85* transgenic mice. Cells from *L2G85* mice constitutively express firefly luciferase and GFP, which allowed us to visualize their location using both in vivo imaging and GFP immunostaining (Sheikh et al., 2007). Cells were transplanted into tibial injuries created in wild-type syngeneic mice. Control mice sustained a tibial injury but received no cell transplant. At various times after grafting, host mice were presented with the luciferin substrate, which is metabolized by luciferase-expressing cells to produce oxyluciferin and energy in the form of light (Shinde et al., 2006). Control mice exhibited no bioluminescence at the injury site (Fig. 3A). By contrast, mice that received an *L2G85* transplant showed a robust bioluminescent signal, which was detectable within 48 hours of cell transplantation and increased with time, peaking at

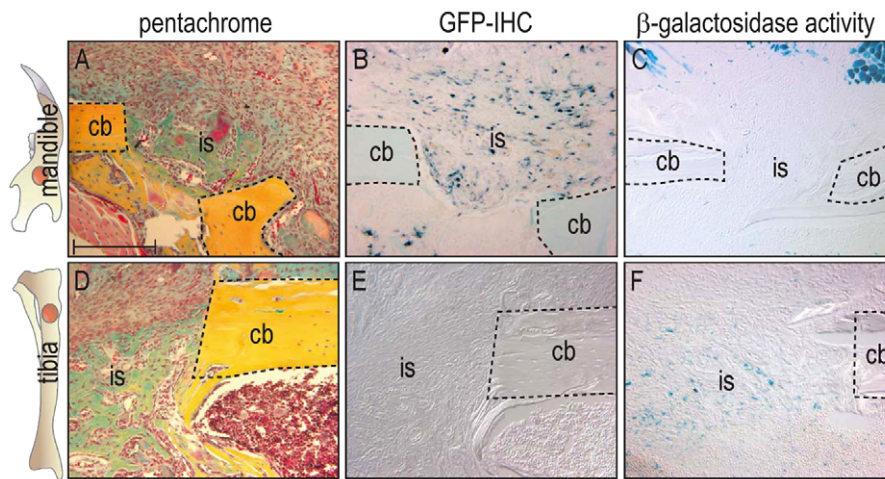


Fig. 2. Skeletal defects heal through recruitment of progenitor cells of their own origin. (A) Pentachrome staining of the mandibular injury site shows bone matrix deposition (blue-green) at post-surgical day 7. (B) GFP-staining reveals that the majority of the cells in the injury site are immunopositive, indicating their neural crest origin. (C) X-Gal staining (a label for mesoderm) is detectable in the surrounding muscle, but is absent in the defect. (D) After 7 days, the tibial defect exhibits a similar amount of osteoid as the mandible. (E) The bony defect is void of GFP-positive neural crest-derived cells. (F) Instead, the defect is occupied by β -galactosidase-positive cells. cb, cortical bone (outlined); is, injury site. Scale bar: 200 μ m.

day 9 (Fig. 3B, and data not shown). The signal gradually tapered off but was still detectable at post-surgery day 23 (Fig. 3C). Between post-surgical days 2 and 9, there was a 7-fold increase in bioluminescence, indicating that luciferase-expressing cells proliferated soon after transplantation.

The gradual reduction in bioluminescence over the course of bone repair suggested that either the transplanted cells died or that they were progressively becoming encased in bone, which then hindered light detection (Fig. 3D,E). To discriminate between these possibilities, we analyzed tissue sections from the injury site. At post-surgical day 7, we found that GFP-positive osteoblasts and osteocytes constituted the vast majority of the callus (Fig. 3F). Thus, we conclude that cells harvested from a donor mouse and transplanted into a syngeneic injury site survive the surgery, proliferate and contribute to the regenerate.

We were now in a position to test whether neural crest-derived and mesoderm-derived osteoprogenitor cells were functionally equivalent. We used periosteum as a source of skeletal progenitor cells and harvested the tissue from tibiae and transplanted it into the mandibular injury sites; we also harvested periosteum from mandibles and transplanted it into tibial injury sites. The transplantation procedures always involved syngeneic hosts and genetically labeled periosteal cells [β -actin GFP (Okabe et al., 1997)] in order to distinguish transplanted cells from host cells. We also performed two additional experiments: one in which tibial periosteum was transplanted into a tibial defect, and one in which mandibular periosteum was transplanted into a mandibular defect. We refer to these as homotopic grafts, because the embryonic origin of the graft matched the origin of the injury site. Homotopic grafts allowed us to evaluate the extent to which transplanted cells contributed to the bony regenerate, as well as the rate and mechanism of healing (i.e. endochondral, intramembranous) following a grafting procedure.

We observed robust bone regeneration in the homotopic grafting experiments. For example, in the tibia ($n=7$; Fig. 4A) and the mandible ($n=7$; Fig. 4C), new bone bridged the defect by day 10. We confirmed that the new bone was derived from the grafted periosteum by GFP immunostaining (Fig. 4B,D). We also determined the volume of new bone by histomorphometry and found that homotopic grafts produced almost equivalent amounts of bone in mandibular and tibial injury sites (Fig. 4I). This latter information demonstrated that both tibial and mandibular injury sites fully supported the differentiation of transplanted progenitor cells into osteoblasts.

We then tested whether neural crest-derived and mesoderm-derived skeletal progenitor cells were interchangeable. When grafts of mandibular periosteum were transplanted into tibial defects (i.e. tibial heterotopic grafts; $n=9$), we observed the same osteogenic effect that we had seen in the homotopic grafting scenario: a bony matrix bridged the defect (Fig. 4E,F). The volume of new bone in this heterotopic grafting experiment, however, exceeded that of both homotopic grafts (Fig. 4I). Was this because the tibial injury supported bone formation better than the mandible, or because the mandibular periosteal cells had a more robust osteogenic potential? The former explanation was unlikely, because both the mandibular and tibial injury sites had nearly equivalent amounts of new bone (Fig. 4I). The latter explanation was more feasible, because mandibular homotopic grafts showed more robust osteogenesis overall (Fig. 4I). The mechanism(s) behind this apparent increase in osteogenic potential of mandibular periosteum became the subject of an additional set of experiments.

If one population of skeletal progenitor cells has 'increased osteogenic potential', this could be attributable to an enhanced rate of proliferation, or an increased rate of differentiation. To distinguish between these possibilities we co-cultured equivalent numbers of neural crest-derived progenitor cells with mesoderm-derived progenitor cells. Cultures were examined at multiple time points and cell numbers counted. From this visual analysis it was clear that mesoderm-derived cells out-proliferated neural crest-derived cells (Fig. 5A,B). BrdU incorporation confirmed that mesoderm-derived osteoprogenitor cells had a significantly greater proliferative potential than neural crest-derived cells (Fig. 5C).

Was there also a difference in the rate of osteogenic differentiation? Both neural crest and mesoderm populations were cultured in osteogenic differentiation media (ODM) and at all time points examined, neural crest-derived cells showed increased Alizarin Red staining (Fig. 5D-F). qRT-PCR assays confirmed this enhanced osteogenic potential: after 4 days in ODM, neural crest-derived cells showed a significant increase in the expression of early osteoblast markers such as *Runx2* and *Colla* (Fig. 5G). After 10 days in ODM, neural crest-derived cells showed significantly higher levels of osteogenic markers including *Runx2*, *Colla*, osteopontin (*Spp1* – Mouse Genome Informatics) and osteocalcin (*Bglap1/2*) (Fig. 5H). Thus, mesoderm-derived skeletal progenitor cells proliferate more, but neural crest-derived skeletal progenitor cells differentiate faster. Therefore, our *in vivo* finding of enhanced osteogenesis in neural crest transplants is explained by the increased osteogenic capacity of neural crest-derived cells.

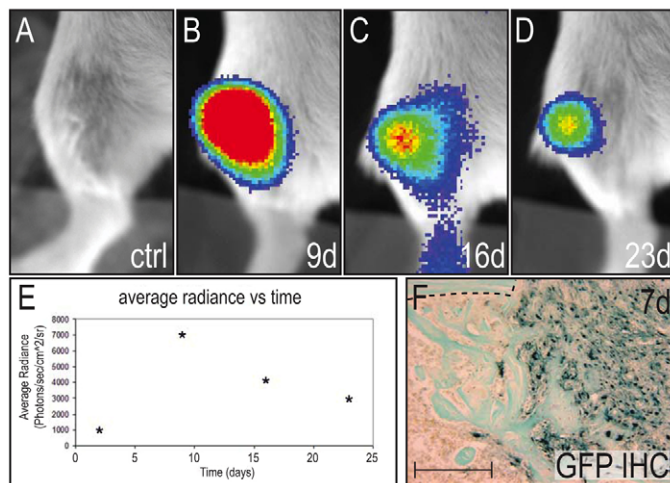


Fig. 3. Bioluminescence imaging demonstrates that cell grafts survive, proliferate and differentiate in vivo. (A) IVIS image of control injury showing no bioluminescence after luciferin injection. (B-E) Time course after L2G85 cell transplantation shows an initial increase of luciferase expression in the injury site, which slowly decreases over time. (F) GFP antibody staining of the injury site at post-surgical day 7 reveals immunopositive osteoblasts and osteocytes. Scale bar: 200 μ m in F.

We returned to our homotopic and heterotopic grafting experiments, and performed one final graft in which tibial periosteum was transplanted into mandibular defects ($n=9$). These mandibular heterotopic grafts showed a different outcome than all of the previous grafts: we found an abundance of cartilage instead of bone in the injury site (Fig. 4G,H,J). Was the cartilage derived from the grafted cells? We performed GFP immunostaining and confirmed that chondrocytes were derived exclusively from β -actin GFP mesodermal cells (Fig. 4K). This finding also confirmed that the transplanted periosteum contains skeletal progenitor cells, because these cells retain their ability to differentiate into chondrocytes and osteoblasts.

In all grafting scenarios, GFP-positive osteocytes and osteoblasts could be detected, which indicated that the transplanted cells were still involved in skeletal regeneration (see Fig. S1A in the supplementary material). Their numbers gradually decreased owing to remodeling of the callus by osteoclasts (see Fig. S1B in the supplementary material). The heterotopic mandibular injuries also showed robust vascularization of the bony region of the callus and a characteristic lack of endothelial cells within the chondrogenic portion of the callus (see Fig. S1C in the supplementary material). Endochondral ossification eventually resulted in the replacement of the GFP-positive cartilage by bone (see Fig. S1D-F in the supplementary material). Collectively, these results indicate that the grafted cells actively participated in the process of skeletal regeneration and that, similar to host cells, they underwent normal remodeling.

Neural crest-derived skeletal progenitor cells adopt a skeletogenic lineage appropriate to their locale

Thus far, our data demonstrate that there are at least two populations of adult skeletal progenitor cells that can be distinguished based on their embryonic origin. Furthermore, neural crest-derived and mesoderm-derived bones heal through the preferential recruitment

of cells from their own embryonic origin. Although this might simply be due to the proximity of one population of progenitor cells, we also demonstrated that in some cases the skeletal progenitor cells are interchangeable. Namely, neural crest-derived osteoprogenitor cells form new bone regardless of whether they were placed into a tibial defect or into another mandibular injury site. Was this because neural crest-derived progenitor cells were committed to an osteogenic fate, which precluded them from adopting a chondrogenic one? We tested this by generating fractures in the mandible, which heal via endochondral ossification. In these cases, neural crest-derived progenitor cells differentiated into chondrocytes (data not shown). Therefore, neural crest-derived progenitor cells exhibit considerable plasticity, even into adulthood: regardless of where they were transplanted, these cells adopted the skeletogenic lineage appropriate to their locale.

An association between embryonic lineage and Hox status might influence skeletal progenitor cell fate

We were still left with the observation that mesoderm-derived skeletal progenitor cells did not appear to exhibit the same plasticity as neural crest-derived skeletal progenitor cells: when they were transplanted into mandibular defects, the grafted mesodermal cells differentiated into chondrocytes even though the environment fully supported osteogenic differentiation (Fig. 4G). These results suggested that there was a fundamental difference in the plasticity of neural crest-derived and mesoderm-derived progenitor cells.

During development, Hox genes are expressed in a nested pattern along the body axis (Chisaka and Capecchi, 1991; Creuzet et al., 2002; Wellik and Capecchi, 2003; Le Douarin et al., 2004), where they provide cells with positional information. For example, *Hoxa11* and *Hoxa13* are expressed in limb mesoderm (Wellik and Capecchi, 2003; Knosp et al., 2004; Rinn et al., 2008), where they regulate patterning and morphogenesis of the fetal appendicular skeleton (Tabin, 1995). Are adult cells provided with positional memory through a similar molecular mechanism? Using in situ hybridization we found that *Hoxa13* and *Hoxa11* expression persisted in the adult skeleton: *Hoxa11* transcripts were readily detectable in tibial osteocytes (Fig. 6A,B) and throughout tibial injuries (Fig. 6C), but were conspicuously absent from the intact or injured mandible (Fig. 6D,E). Our subsequent analyses focused on *Hoxa11* because of its exclusive expression in the tibia and absence from the mandible.

Embryonic cell transplantation experiments have shown that Hox gene expression is a critical determinant of whether grafted cells integrate into their new location (reviewed by Le Douarin et al., 2004). Did a discrepancy in Hox expression underlie the chondrogenic outcome of the adult heterotopic grafts? We harvested Hox-positive tibial periosteum and transplanted it into the Hox-negative mandible, then evaluated the status of Hox gene expression in the injury site. After 7 days, we found that the grafted cells maintained their *Hoxa11*-positive status, and the injury site sustained its *Hoxa11*-negative status (Fig. 6F,G). Furthermore, the domain of *Hoxa11* expression coincided precisely with the chondrogenic region in the heterotopic callus (Fig. 6F,G).

Embryonic studies have shown that when Hox-negative tissues are transplanted they adopt the Hox status of their new location (Itasaki et al., 1996). We examined the tibial heterotopic transplants to see whether the same kind of change occurred in an adult regenerative context. At the time of harvest, mandibular periosteum was Hox-negative (Fig. 6D), but when examined at post-transplantation day 7 the grafted cells expressed *Hoxa11* (Fig. 6H,I). Was this just an artifact of the transplantation procedure, or were the

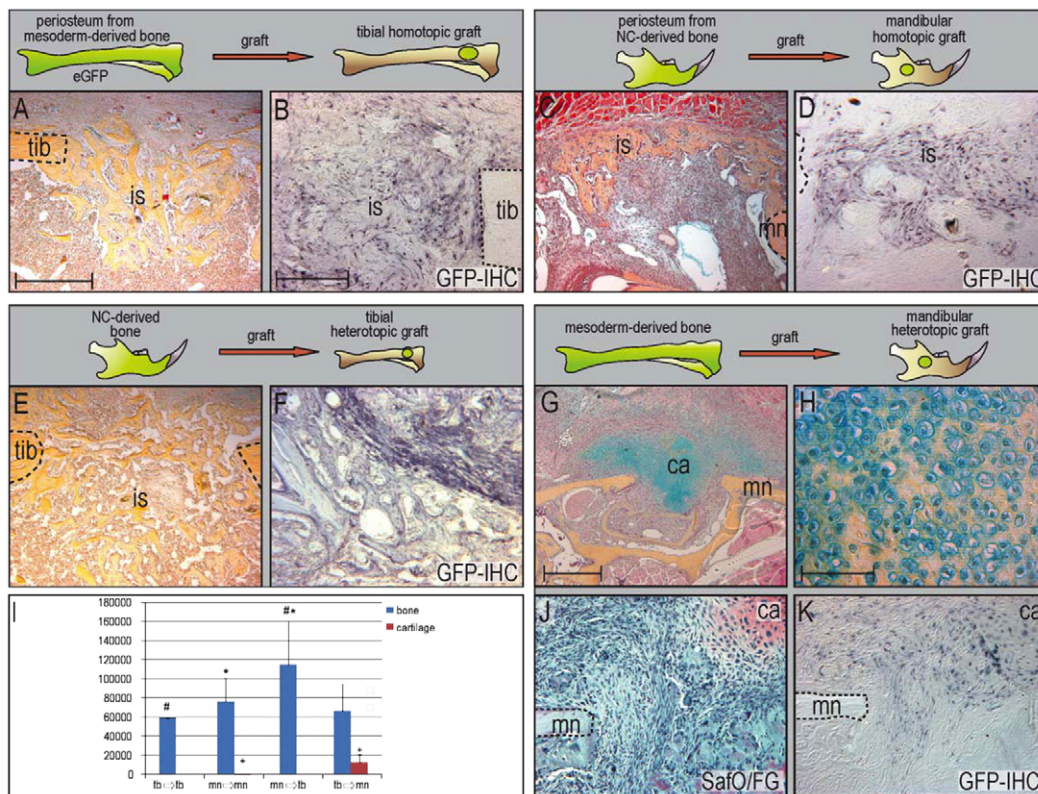


Fig. 4. Embryonic origin of the graft influences cell fate decision in a transplantation assay. (A) Pentachrome staining shows that the homotypic transplantation of tibial periosteum into a tibial defect results in robust bone formation through intramembranous ossification at post-surgical day 10. (B) GFP antibody staining reveals that the majority of the regenerate is derived from the grafted periosteum. (C,D) Similarly, the homotypic graft of mandibular periosteum into a mandibular injury induces direct differentiation into bone (C) and, again, the majority of the regenerate is derived from the GFP-positive graft (D). (E) Placement of neural crest-derived periosteum into a mesoderm-derived injury site results in intramembranous bone formation. (F) GFP immunohistochemistry confirmed that the grafted cells are actively committed to the healing response. (G) However, when tibial periosteum is transplanted into a mandible, the cells undergo endochondral ossification. (H) High magnification of the cartilage condensation reveals that the cells are undergoing hypertrophy. (I) Histomorphometry of the four grafting scenarios; see Materials and methods for details. *, # and + indicate significant differences; $P \leq 0.01$. (J,K) Safranin O/Fast Green staining and GFP immunohistochemistry show the spatial correlation of chondrogenesis and the graft. ca, cartilage; is, injury site; mn, mandible; tib, tibia. Scale bar: 200 μm in A,C,E; 100 μm in B,D,F,J,K; 400 μm in G; 50 μm in H.

Hox-positive host cells responsible for this switch in molecular fate? We co-cultured *Hoxa11*-expressing tibial periosteal cells (Fig. 6J,K) with Hox-negative mandibular periosteal cells and found that within 5 days the formerly Hox-negative mandibular periosteal cells began to express *Hoxa11* (Fig. 6L,M).

Thus, cranial neural crest cells respond to local cues, adopt the Hox status of their new locale, and robustly contribute to the formation of a bony regenerate. By contrast, mesodermal cells maintain their Hox status when grafted into the mandible. This mismatch between the Hox status of the graft and the injury site correlated with a disruption in bone regeneration, such that the grafted cells failed to differentiate into osteoblasts (Fig. 7). Therefore, embryonic origin, as well as Hox expression status, distinguishes neural crest-derived from mesoderm-derived skeletal progenitor cells, and both characteristics have an influence on the fate of skeletal progenitor cells in a regenerative context.

DISCUSSION

At a histological level, cranial skeletal repair is indistinguishable from long-bone repair. Both injury sites are vascularized to a similar extent following trauma; both become populated by skeletal progenitor cells; both show evidence of a bony matrix that

undergoes extensive remodeling; and both heal the defect within a similar time frame. Thus, from a histological perspective, the healing of a cranial neural crest-derived skeletal element is no different from healing in a mesoderm-derived element.

Our cellular and molecular analyses belie this histological equivalency. Using *Wnt1Cre::Z/EG* mice we found that when the neural crest-derived mandible is injured, the callus is composed entirely of neural crest-derived cells. In parallel, we found that when the tibia is damaged, the injury site is occupied entirely by mesoderm-derived cells. Thus, there are at least two populations of adult skeletal progenitor cells that can be distinguished based on their embryonic origins.

Injured skeletal elements normally use cells of their own embryonic origin for repair. At least in the mandibular repair site, we found no evidence of cells from the circulation that contributed in a major way to the repair process. Likewise, we did not observe a major contribution from endothelial cells, which in the head are derived from mesoderm (Couly et al., 1995). The presence of two distinct populations of skeletal stem cells in the adult might have clinical implications because if bones preferentially heal using cells that share the same embryonic origin, then reparative strategies may have to take this variable into account in order to be maximally effective.

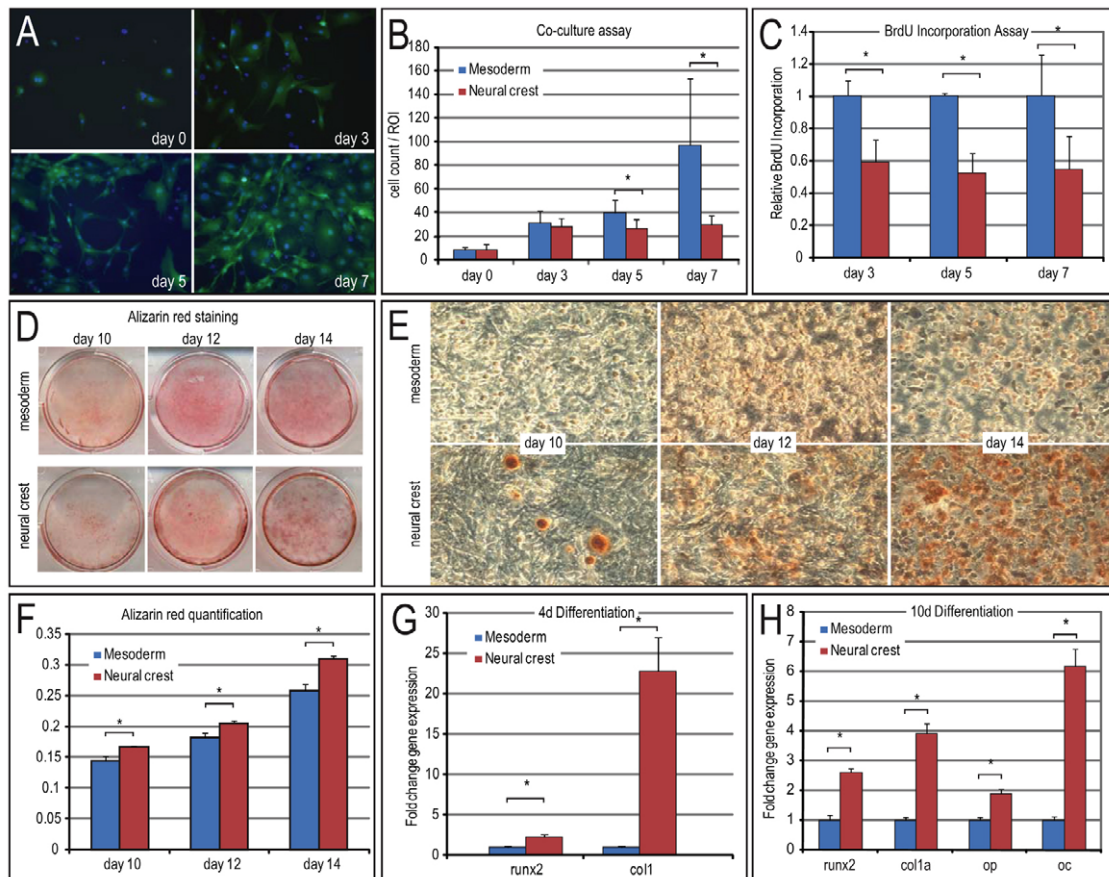


Fig. 5. Neural crest-derived and mesoderm-derived periosteal cells have distinct proliferation and osteogenic differentiation potentials. (A) Skeletal progenitor cells from the mandibular periosteum and GFP-positive tibial periosteum were co-cultured for 0, 3, 5 and 7 days; cell nuclei were labeled with Hoechst and viewed using fluorescent imaging. (B) Quantification of the co-culture showed a linear increase in the number of GFP-positive mesoderm-derived cells and only a minor increase in the number of neural crest-derived cells. (C) BrdU incorporation assay at 3, 5 and 7 days showed higher proliferation rates for mesoderm-derived cells at all time points. (D,E) Alizarin Red staining of mesoderm-derived and neural crest-derived skeletal progenitor cell cultures after 10, 12 and 14 days in osteogenic differentiation media. (F) Quantification of Alizarin Red mineralization showed a statistically significant increase in the amount of mineralized matrix in neural crest-derived samples. (G) qRT-PCR performed on RNA isolated from cell populations after 4 days in vitro. Neural crest-derived cells showed an increase in the expression of *Runx2* and *Col1a*. (H) qRT-PCR performed on RNA isolated from cell populations after 10 days in vitro demonstrated that neural crest-derived cells showed an increase in the expression of all osteogenic markers, including *Runx2*, osteopontin (op), *Col1a* and osteocalcin (oc). * $P \leq 0.01$.

But does the fact that mandibular defects heal via neural crest-derived progenitor cells, and tibial defects heal via mesoderm-derived progenitors, indicate a preferential recruitment? Or are cells from the local environment merely conscripted to aid in the reparative process, and it just happens that these cells that contribute to the regenerate share the same embryonic origin as the damaged bone? This latter possibility would suggest that despite differences in embryonic origin, cranial and appendicular bones can heal using any skeletal progenitor cell population.

We directly tested this possibility by transplanting tibial and mandibular skeletal progenitor cells into heterotopic wound sites. Whereas neural crest-derived skeletal progenitor cells integrated and contributed to the bony regenerate in either location, mesoderm-derived progenitor cells differentiated into chondrocytes when they were placed in the mandibular defect. Why didn't mesoderm-derived progenitor cells differentiate into osteoblasts in this locale? We tested whether the difference in neural crest-derived and mesoderm-derived progenitor cells reflected a disparity between how bones form, but we found that the mandible and tibia are not

restricted to any single type of repair based on their embryonic origin. Long bones form through endochondral ossification and facial bones form through intramembranous ossification, but both bones can heal through either mechanism (Ferguson et al., 1998; Ferguson et al., 1999).

The mechanical environment also influences how bones heal and we wondered whether this might have contributed to the chondrogenic differentiation of mesoderm-derived progenitors placed into a mandibular defect. Irrespective of the embryonic origin of a bone, however, a stabilized environment favors intramembranous ossification, whereas a non-stabilized environment heals through endochondral ossification (reviewed by Carter et al., 1998). In our injury model, the mechanical environment was equivalent. Therefore, we cannot attribute the disparity in healing to differences in the mechanical environment.

We sought a molecular explanation for this phenomenon, and examined the injury sites for alterations in gene expression. Once cells had begun the process of osteoblast differentiation, however, there was no discernible difference in their expression patterns.

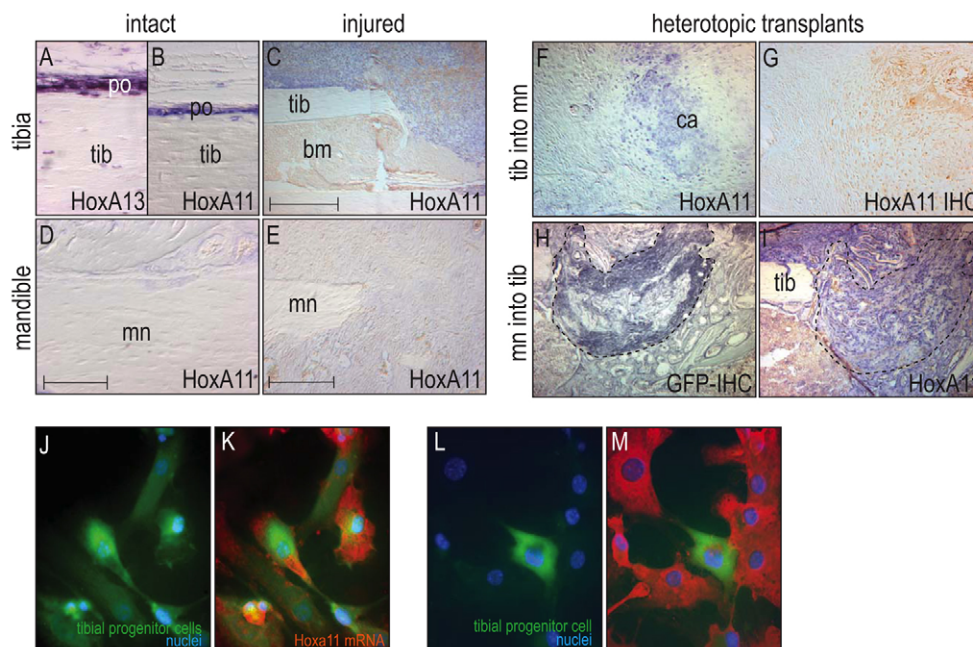


Fig. 6. Hox-negative neural crest skeletal progenitor cells assume a Hox-positive status when placed into a Hox-positive environment.

(A,B) The adult tibial periosteum expresses *Hoxa13* and *Hoxa11*. (C) At post-surgical day 3, the tibial injury site is occupied by *Hoxa11*-expressing cells. (D,E) By contrast, the mandibular periosteum is devoid of *Hoxa11* expression (D), and injury does not induce *Hoxa11* expression (E). (F,G) Hox-positive tibial periosteum maintains its expression when transplanted into a Hox-negative mandibular injury site. (H) GFP antibody staining labels Hox-negative mandibular periosteum in a tibial injury site. (I) Adjacent section shows *Hoxa11* expression in the transplanted mandibular periosteum (dashed line). (J,K) Skeletal progenitor cells derived from β -actin GFP tibial periosteum express GFP (J) and *Hoxa11* (K). (L,M) When these GFP-positive, Hox-positive cells were co-cultured with Hox-negative neural crest-derived cells (L) the formerly Hox-negative mandibular cells begin to express *Hoxa11* (M). bm, bone marrow; ca, cartilage; mn, mandible; po, periosteum; tib, tibia. Scale bar: 50 μ m in A,B,D,F,G; 100 μ m in E; 200 μ m in C,H,I.

What we searched for was a difference in ‘molecular identity’ between the two populations of osteoprogenitor cells, which led us to consider Hox gene expression.

We reasoned that tissues that undergo continual remodeling must have a mechanism whereby stem/progenitor cells are informed of their ancestors’ phenotypic identity. One mechanism by which this might be accomplished is via Hox gene expression, and we took cues from the developmental expression pattern of Hox genes to focus our analyses. Limb mesenchyme destined to form the tibiae expresses a number of Hox genes including *Hox11* (Wellik and Capecchi, 2003), and we found that *Hoxa11* expression persisted in adult tibial osteoblasts and osteocytes (Fig. 6). *Hoxa11* was not expressed in the adult mandible (Fig. 6), in keeping with its Hox-negative status during embryonic development (Creuzet et al., 2002).

The absence of *Hoxa11* expression in the mandible was especially important in our next experiments, in which we examined the heterotopic grafts for their Hox status. Tibial grafts maintained their Hox-positive status even after transplantation into a Hox-negative mandibular environment. Hox-negative neural crest-derived progenitors, by contrast, adopted Hox expression when transplanted into a Hox-positive location. Our in vitro data parallel these in vivo findings: Hox-negative neural crest-derived cells adopted a Hox code after co-culture with Hox-expressing mesoderm-derived cells, and these mesodermal cells did not alter their Hox-positive status. Thus, adult skeletal stem cells are equipped with a type of positional memory that is retained even after transplantation. This conclusion is not without precedent: when embryonic Hox-negative cranial neural crest cells are transplanted into a Hox-positive domain within the neural tube, the cells adopt the Hox status in their new

environment; conversely, Hox-positive cells maintain their Hox status when transplanted into a Hox-negative environment (Grapin-Botton et al., 1995; Couly et al., 1998).

These and additional experiments indicate that the Hox status of a cell confers upon it a sense of positional identity, and this identity is unchanged when cells are placed into a new environment (Le Douarin et al., 2004). There is a ‘flip side’ to this: mandibular neural crest cells normally lack Hox gene expression and this ‘Hox-free’ condition has been strongly associated with their remarkable plasticity in development and evolution (reviewed by Helms et al., 2005).

Other groups have evaluated the correlation between Hox expression and the skeletogenic capacity of a cell (Abzhanov et al., 2003), but these experiments are difficult to compare with our findings. First, our experiments were largely conducted in vivo, whereas the majority of those analyses were carried out in vitro. Second, our data do not implicate Hox status in influencing whether a cell population has skeletogenic capacity or not. Instead, we show that Hox expression seems to confer a positional memory on adult cells, which closely parallels the function of Hox genes during embryonic development.

We found that Hox-negative adult neural crest cells begin to express posterior Hox genes when placed into a Hox-positive environment. This is a very intriguing finding because it implies that injury sites have specific Hox codes, and a synchrony between the cells occupying the injury site and the injury environment itself might be a crucial component of normal healing. How is such a Hox code established in a wound? Future experiments will directly test whether a disparity in Hox gene expression underlies the ability of any grafted cell to heal wounds more efficiently.

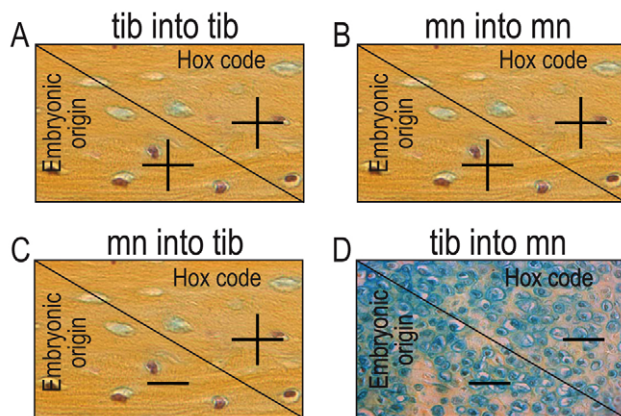


Fig. 7. Scheme of interactions between embryonic origin and Hox status during adult bone regeneration in mouse. (A,B) In a homotopic tibial or mandibular graft, both embryonic origin and Hox code are equal (+), which leads to osteogenic differentiation of osteoprogenitor cells. (C) When mandibular periosteum is transplanted into a tibial injury, the embryonic origin of the graft and recipient are different (-). Hox expression, however, is the same in graft and recipient because the grafted cells, which are initially Hox-negative, turn on Hox expression when placed into the Hox-positive environment. (D) In the mandibular heterotopic graft, the embryonic origin of graft and recipient are different, and the Hox status of the graft and host remain unequal, which results in chondrogenic differentiation of the osteoprogenitor cells. mn, mandible; tib, tibia.

Other adult cells use a Hox code to distinguish their position in the body: dermal fibroblasts retain the Hox code appropriate to their site of initial derivation despite numerous passages in culture (Chang et al., 2002; Rinn et al., 2008). Furthermore, Hox-positive fibroblasts do not alter their regional Hox code even when cells from different locales are cultured together (Rinn et al., 2008). Those experiments, however, did not evaluate fibroblasts from the head. Are cranial neural crest-derived dermal fibroblasts, like neural crest-derived skeletal progenitor cells, Hox-negative? If so, do they readily adopt the Hox status when co-cultured or transplanted as we have shown here for skeletal progenitor cells?

A wider implication of these findings is that although progenitor cells in different parts of the body produce similar kinds of tissues (bone, skin), the success or failure of a graft might be controlled by molecular features that distinguish one type of progenitor cell from another. The histological characteristics of skin grafts are carefully considered prior to grafting; perhaps the molecular characteristics should be as well. Currently, most bone grafting procedures performed for craniofacial applications use cells derived from the mesodermal lineage (e.g. the fibula, iliac crest, ribs) and these are less effective than grafts composed of cells derived from the neural crest (D'Addona and Nowzari, 2001). Clearly, further studies are needed to directly test whether the molecular differences between a graft and the recipient site are critical determinants of successful tissue repair and regeneration.

We thank Yu-Jin Park for outstanding technical assistance and Chris Contag for providing the *L2G85* mice. This work was supported by NIH RO1 PA-02-011, NIH RO1 AR45989 and the Air Force Office of Research (FOS-2004-0025A).

Supplementary material

Supplementary material for this article is available at <http://dev.biologists.org/cgi/content/full/135/17/2845/DC1>

References

- Abzhanov, A., Tzahor, E., Lassar, A. B. and Tabin, C. J. (2003). Dissimilar regulation of cell differentiation in mesencephalic (cranial) and sacral (trunk) neural crest cells in vitro. *Development* **130**, 4567-4579.
- Albrecht, U. E. G., Helms, J. A. and Lin, H. (1997). Visualization of gene expression patterns by in situ hybridization. In *Molecular and Cellular Methods in Developmental Toxicology* (ed. G. P. Daston), pp. 23-48. Boca Raton, FL: CRC Press.
- Carter, D. R., Beaupré, G. S., Giori, N. J. and Helms, J. A. (1998). Mechanobiology of skeletal regeneration. *Clin. Orthop. Relat. Res.* **82**, S41-S55.
- Chai, Y., Jiang, X., Ito, Y., Bringas, P., Jr, Han, J., Rowitch, D. H., Soriano, P., McMahon, A. P. and Sucov, H. M. (2000). Fate of the mammalian cranial neural crest during tooth and mandibular morphogenesis. *Development* **127**, 1671-1679.
- Chang, H. Y., Chi, J. T., Dudoit, S., Bondre, C., van de Rijn, M., Botstein, D. and Brown, P. O. (2002). Diversity, topographic differentiation, and positional memory in human fibroblasts. *Proc. Natl. Acad. Sci. USA* **99**, 12877-12882.
- Chisaka, O. and Capecchi, M. (1991). Regionally restricted developmental defects resulting from targeted disruption of the mouse homeobox gene *hox1.5*. *Nature* **350**, 473-479.
- Clifford, D. H. (1984). Preanesthesia, anesthesia, analgesia, and euthanasia. In *Laboratory Animal Medicine ACLAM Series* (ed. J. G. Fox et al.), pp. 527-562. New York: Academic Press.
- Colnot, C., Thompson, Z., Miclau, T., Werb, Z. and Helms, J. A. (2003). Altered fracture repair in the absence of MMP9. *Development* **130**, 4123-4133.
- Colnot, C., Romero, D. M., Huang, S. and Helms, J. A. (2005). Mechanisms of action of demineralized bone matrix in the repair of cortical bone defects. *Clin. Orthop. Relat. Res.* **435**, 69-78.
- Couly, G. F., Coltey, P. M. and Le Douarin, N. M. (1993). The triple origin of skull in higher vertebrates: a study in quail-chick chimeras. *Development* **117**, 409-429.
- Couly, G., Coltey, P., Eichmann, A. and Le Douarin, N. M. (1995). The angiogenic potentials of the cephalic mesoderm and the origin of brain and head blood vessels. *Mech. Dev.* **53**, 97-112.
- Couly, G., Grapin-Botton, A., Coltey, P., Ruhin, B. and Le Douarin, N. M. (1998). Determination of the identity of the derivatives of the cephalic neural crest: incompatibility between Hox gene expression and lower jaw development. *Development* **125**, 3445-3459.
- Creuzet, S., Couly, G., Vincent, C. and Le Douarin, N. M. (2002). Negative effect of Hox gene expression on the development of the neural crest-derived facial skeleton. *Development* **129**, 4301-4313.
- Cumano, A. and Godin, I. (2007). Ontogeny of the hematopoietic system. *Annu. Rev. Immunol.* **25**, 745-785.
- D'Addona, A. and Nowzari, H. (2001). Intramembranous autogenous osseous transplants in aesthetic treatment of alveolar atrophy. *Periodontol.* **2000** **27**, 148-161.
- D'Amico-Martel, A. and Noden, D. M. (1983). Contributions of placodal and neural crest cells to avian cranial peripheral ganglia. *Am. J. Anat.* **166**, 445-468.
- Danielian, P. S., Muccino, D., Rowitch, D. H., Michael, S. K. and McMahon, A. P. (1998). Modification of gene activity in mouse embryos in utero by a tamoxifen-inducible form of Cre recombinase. *Curr. Biol.* **8**, 1323-1326.
- Ferguson, C. M., Miclau, T., Hu, D., Alpern, E. and Helms, J. A. (1998). Common molecular pathways in skeletal morphogenesis and repair. *Ann. N.Y. Acad. Sci.* **857**, 33-42.
- Ferguson, C., Alpern, E., Miclau, T. and Helms, J. A. (1999). Does adult fracture repair recapitulate embryonic skeletal formation? *Mech. Dev.* **87**, 57-66.
- Gerstenfeld, L. C., Cullinane, D. M., Barnes, G. L., Graves, D. T. and Einhorn, T. A. (2003). Fracture healing as a post-natal developmental process: Molecular, spatial, and temporal aspects of its regulation. *J. Cell Biochem.* **88**, 873-884.
- Grapin-Botton, A., Bonnin, M., McNaughton, L. A., Krumlauf, R. and Douarin, N. M. L. (1995). Plasticity of transposed rhombomeres: Hox gene induction is correlated with phenotypic modifications. *Development* **121**, 2707-2721.
- Helms, J. A., Cordero, D. and Tapadia, M. D. (2005). New insights into craniofacial morphogenesis. *Development* **132**, 851-861.
- Itasaki, N., Sharpe, J., Morrison, A. and Krumlauf, R. (1996). Reprogramming Hox expression in the vertebrate hindbrain: influence of paraxial mesoderm and rhombomere transposition. *Neuron* **16**, 487-500.
- Jiang, X., Rowitch, D. H., Soriano, P., McMahon, A. P. and Sucov, H. M. (2000). Fate of the mammalian cardiac neural crest. *Development* **127**, 1607-1616.
- Joseph, N. M., Mukoyama, Y. S., Mosher, J. T., Jaegle, M., Crone, S. A., Dormand, E. L., Lee, K. F., Meijer, D., Anderson, D. J. and Morrison, S. J. (2004). Neural crest stem cells undergo multilineage differentiation in developing peripheral nerves to generate endoneurial fibroblasts in addition to Schwann cells. *Development* **131**, 5599-5612.
- Kim, J. B., Leucht, P., Luppen, C. A., Park, Y. J., Beggs, H. E., Damsky, C. H. and Helms, J. A. (2007a). Reconciling the roles of FAK in osteoblast differentiation, osteoclast remodeling, and bone regeneration. *Bone* **41**, 39-51.

- Kim, J. B., Leucht, P., Lam, K., Luppen, C., Ten Berge, D., Nusse, R. and Helms, J. A. (2007b). Bone regeneration is regulated by wnt signaling. *J. Bone Miner. Res.* **22**, 1913-1923.
- Knosp, W. M., Scott, V., Bachinger, H. P. and Stadler, H. S. (2004). HOXA13 regulates the expression of bone morphogenetic proteins 2 and 7 to control distal limb morphogenesis. *Development* **131**, 4581-4592.
- Le Douarin, N. M. and Dupin, E. (1993). Cell lineage analysis in neural crest ontogeny. *J. Neurobiol.* **24**, 146-161.
- Le Douarin, N. M., Cruzet, S., Couly, G. and Dupin, E. (2004). Neural crest cell plasticity and its limits. *Development* **131**, 4637-4650.
- Leucht, P., Kim, J. B., Wazen, R., Currey, J. A., Nanci, A., Brunski, J. B. and Helms, J. A. (2007). Effect of mechanical stimuli on skeletal regeneration around implants. *Bone* **40**, 919-930.
- Leucht, P., Kim, J. B. and Helms, J. A. (2008). Beta-catenin-dependent Wnt signaling in mandibular bone regeneration. *J. Bone Joint Surg. Am.* **90 Suppl. 1**, 3-8.
- Nagoshi, N., Shibata, S., Kubota, Y., Nakamura, M., Nagai, Y., Satoh, E., Morikawa, S., Okada, Y., Mabuchi, Y., Katoh, H. et al. (2008). Ontogeny and multipotency of neural crest-derived stem cells in mouse bone marrow, dorsal root ganglia, and whisker pad. *Cell Stem Cell* **2**, 392-403.
- Noden, D. M. (1982). Patterns and Organization of Craniofacial Skeletogenic Mesenchyme: A Perspective. In *Factors and Mechanisms Influencing Bone Growth* (eds A. D. Dixon and B. G. Sarnat). New York: Alan R. Liss.
- Novak, A., Guo, C., Yang, W., Nagy, A. and Lobe, C. G. (2000). Z/EG, a double reporter mouse line that expresses enhanced green fluorescent protein upon Cre-mediated excision. *Genesis* **28**, 147-155.
- Okabe, M., Ikawa, M., Kominami, K., Nakanishi, T. and Nishimune, Y. (1997). 'Green mice' as a source of ubiquitous green cells. *FEBS Lett.* **407**, 313-319.
- Rinn, J. L., Wang, J. K., Allen, N., Brugmann, S. A., Mikels, A. J., Liu, H., Ridky, T. W., Stadler, H. S., Nusse, R., Helms, J. A. et al. (2008). A dermal HOX transcriptional program regulates site-specific epidermal fate. *Genes Dev.* **22**, 303-307.
- Seeman, E. and Delmas, P. D. (2006). Bone quality-the material and structural basis of bone strength and fragility. *New Engl. J. Med.* **354**, 2250-2261.
- Sheehan, D. C. and Hrapchak, B. B. (1980). *Theory and Practice of Histotechnology*. Columbus, Ohio: Batelle Press.
- Sheikh, A. Y., Lin, S. A., Cao, F., Cao, Y., van der Bogt, K. E., Chu, P., Chang, C. P., Contag, C. H., Robbins, R. C. and Wu, J. C. (2007). Molecular imaging of bone marrow mononuclear cell homing and engraftment in ischemic myocardium. *Stem Cells* **25**, 2677-2684.
- Shinde, R., Perkins, J. and Contag, C. H. (2006). Luciferin derivatives for enhanced in vitro and in vivo bioluminescence assays. *Biochemistry* **45**, 11103-11112.
- Tabin, C. (1995). The initiation of the limb bud: growth factors, Hox genes, and retinoids. *Cell* **80**, 671-674.
- Wellik, D. M. and Capecchi, M. R. (2003). Hox10 and Hox11 genes are required to globally pattern the mammalian skeleton. *Science* **301**, 363-367.